atmosphere

Article

Weekly VPD and Monthly Precipitation as Contrasting Dominant Drivers of Soil Moisture in the Yangtze River Basin

Yucheng Liu [1], Ran Huo [1,*], Bowen Zhu [1] and Lele Deng [2]

[1] College of Water Resource Science and Engineering, Taiyuan University of Technology, Taiyuan 030024, China
[2] Hubei Key Laboratory of Intelligent Yangtze and Hydroelectric Science, China Yangtze Power Co., Ltd., Yichang 443002, China
* Correspondence: huoran@tyut.edu.cn

Abstract

Soil moisture is a key indicator of agricultural and hydrological drought, but its meteorological controls vary across temporal scales. Using ESA CCI soil moisture products from 2010 to 2022, this study investigated soil moisture variability in the Yangtze River Basin at weekly, monthly, and annual scales. The product was first validated using ground observations and ERA5 reanalysis data, and a generalized additive model (GAM) was then applied to quantify the relative contributions of precipitation, temperature, wind speed, and VPD under normal conditions and during three extreme drought events. The validation showed that ESA CCI soil moisture captured basin-scale variations well, with mean absolute deviations of 0.0460, 0.0434, and 0.0072 m^3/m^3 in the upper, middle, and lower reaches, respectively, and a basin-wide RMSE of 0.0127 m^3/m^3 against ERA5. The attribution results revealed a clear scale-dependent shift in soil moisture controls. At the weekly scale, VPD dominated soil moisture variability, with a basin-wide average contribution of 47.04% and a maximum contribution of 55.92% in the lower reaches, indicating that short-term soil drying is mainly driven by VPD. At the monthly scale, precipitation became the primary control, with a basin-wide average contribution of 36.62% and a maximum contribution of 44.65% in the upper reaches, reflecting the role of accumulated rainfall recharge in maintaining soil moisture storage. During extreme drought events, the monthly-scale dominance of precipitation weakened, and precipitation, VPD, temperature, and wind speed each contributed approximately 20–30%, suggesting that drought development results from the combined effects of reduced water input and enhanced atmospheric water loss. These findings indicate that precipitation-based drought monitoring may underestimate rapid soil drying risks, whereas incorporating atmospheric demand indicators such as VPD can improve drought early warning and water resource management under a warming climate.

Keywords: ESA CCI surface soil moisture; multiscale soil moisture dynamics; precipitation recharge; vapor pressure deficit; generalized additive model; Yangtze River Basin

Check for updates

Academic Editor: Jimmy O. Adegoke

Received: 1 July 2026
Revised: 2 August 2026
Accepted: 7 August 2026
Published: 13 August 2026

1. Introduction

Soil moisture is a direct indicator of terrestrial water availability and plays an essential role in drought development, agricultural production, ecosystem stability, and basin-scale water resource management [1]. By regulating precipitation infiltration, surface runoff, evapotranspiration, and vegetation water supply, soil moisture links atmospheric, surface, and subsurface hydrological processes [2]. Under global climate change and intensified human activities, regional hydroclimatic conditions have become increasingly variable.

Changes in precipitation regimes and rising atmospheric evaporative demand can directly affect soil moisture dynamics [3,4]. Human activities can also modify soil moisture processes through irrigation, land-use change, and afforestation. Irrigation increases soil moisture inputs in agricultural areas, land-use change affects infiltration, surface runoff, and evapotranspiration, and afforestation alters canopy interception, root water uptake, and soil moisture retention [5]. These changes can further influence runoff generation, vegetation productivity, and ecosystem services, thereby increasing the risk of agricultural and hydrological drought [6,7]. Therefore, understanding how soil moisture varies and identifying the factors that control soil moisture depletion are important for drought monitoring and water security assessment.

Previous studies have improved our understanding of soil moisture from several perspectives. Land-atmosphere feedback studies have shown that soil moisture anomalies can regulate regional water and energy exchanges and further influence drought development under climate warming [2,8]. Vegetation-related studies have demonstrated that canopy processes and root-zone water uptake can redistribute soil moisture and alter hydrological fluxes [9]. Terrain and soil-property studies have further revealed that topographic attributes and porous media conditions contribute to the Spatial disparities of soil moisture [10]. In terms of data sources, ground-based observation networks provide reliable local measurements, but their spatial coverage is often sparse and may not fully represent complex terrain or ecologically vulnerable regions [11,12]. Satellite remote sensing products, such as SMAP, SMOS, AMSR2, Fengyun-series products, and ESA CCI SM, have therefore become important tools for regional and global soil moisture monitoring because they provide continuous spatial coverage and long-term observational records [13–16]. Among these products, ESA CCI SM is well suited for long-term basin-scale analysis because it integrates multi-sensor observations and provides relatively continuous records for examining soil moisture variability over large spatial domains [15].

In this study, precipitation, temperature, wind speed, and VPD were selected because they represent water supply, thermal conditions, turbulent exchange, and atmospheric evaporative demand, respectively. Precipitation replenishes soil moisture through infiltration, while temperature affects evapotranspiration and soil evaporation by regulating surface energy conditions. Wind speed influences turbulent water vapor transport near the land surface, and VPD reflects atmospheric water demand and is closely associated with rapid soil moisture depletion [17–20]. However, the relative importance of these factors is not constant. Accumulated precipitation may dominate soil moisture recharge at monthly or longer scales, whereas short-term soil moisture depletion may be more strongly controlled by atmospheric evaporative demand. Although land-atmosphere feedbacks, vegetation dynamics, terrain conditions, and soil properties have all been shown to influence soil moisture variability, the way in which dominant meteorological controls shift across temporal scales remains insufficiently quantified in the Yangtze River Basin [21].

Despite these advances, several limitations remain. Land surface models provide continuous spatial coverage, but their estimates may contain uncertainties in regions strongly affected by irrigation, reservoir regulation, and land-use change. Ground observations provide accurate site-scale measurements, but their spatial representativeness is often limited by sparse station distribution, complex terrain, and ecologically sensitive landscapes [11,12]. Remote sensing soil moisture products offer an effective alternative for basin-scale and long-term monitoring, yet many remote-sensing-based studies still focus on a single temporal scale or long-term average conditions [13–16]. As a result, cross-scale comparisons of soil moisture dynamics remain limited. In addition, previous attribution studies have mainly emphasized precipitation and temperature, whereas VPD and wind speed have received less attention. Traditional linear methods may also be inadequate for detecting nonlinear responses between soil moisture and meteorological factors under extreme drought stress [21,22].

These limitations highlight several unresolved issues. The scale-dependent variation in the dominant controls of soil moisture across weekly, monthly scales remains insufficiently quantified in the Yangtze River Basin. The relative contributions of atmospheric evaporative demand and turbulent exchange, represented by VPD and wind speed, to soil moisture depletion are still less clearly understood than those of precipitation and temperature. It also remains uncertain whether the dominant meteorological controls identified under normal conditions remain valid during extreme drought events in the basin. Resolving these issues is necessary for improving the process-based understanding of soil moisture depletion and for strengthening drought monitoring and early-warning capacity in the Yangtze River Basin.

GAM provides a useful framework for addressing these issues because they can capture nonlinear relationships while maintaining relatively clear interpretability [23]. For example, Abolafia-Rosenzweig applied GAMs to high-resolution summer drought forecasting in the western United States and showed their usefulness in linking drought occurrence with antecedent climatic and hydrological conditions [24]. Li used a GAM framework to identify the dominant drivers of satellite-observed global soil moisture variability from 2001 to 2020, showing that vapor pressure deficit was the primary driver at short temporal scales, whereas precipitation exerted stronger control at monthly scales in some regions [21]. Regional studies based on ERA5-Land soil moisture have also used GAMs to quantify the individual and combined effects of precipitation, evaporation, temperature, and vegetation conditions on soil moisture variability. However, previous GAM-based studies have mainly focused on global-scale assessments, drought forecasting, or monthly-scale attribution. Few studies have examined how meteorological controls of soil moisture shift across weekly, monthly, and annual scales in the Yangtze River Basin, especially during extreme drought events. Therefore, GAMs are suitable for this study because they can describe nonlinear and potentially threshold-like soil moisture responses while retaining the interpretability needed to identify dominant drivers.

The Yangtze River Basin is one of China's most important agricultural production regions and ecological security barriers [25]. In recent decades, however, the basin has experienced increasingly frequent and severe drought events. The 2011 spring–summer drought caused substantial shrinkage of major lakes such as Poyang Lake and Dongting Lake, while the 2013 high-temperature drought produced severe heat stress, large precipitation deficits, and extensive crop losses. The prolonged drought in 2019 also affected large agricultural areas in Jiangxi and Anhui Provinces. These events threatened water supply, food production, ecosystem stability, and regional socioeconomic development [26,27]. Although drought characteristics in the Yangtze River Basin have been widely investigated, two issues remain unclear: whether the dominant drivers of soil moisture under normal conditions also operate during extreme drought events, and whether these drivers differ across weekly and monthly scales.

To address these gaps, this study used ESA Climate Change Initiative Soil Moisture products from 2010 to 2022 to investigate soil moisture dynamics in the Yangtze River Basin. The novelty of this study lies in its integrated assessment of ESA CCI soil moisture applicability, multi-temporal-scale soil moisture variability, and nonlinear meteorological attribution under both normal and extreme drought conditions in the Yangtze River Basin. The objectives were to: (1) evaluate the applicability of the ESA CCI soil moisture product in the basin using ground observations and reanalysis data as a prerequisite for the subsequent multiscale analyses of soil moisture variation and the relative contributions of meteorological factors; (2) analyze the temporal and spatial variation patterns of soil moisture at weekly, monthly, and annual scales across the upper, middle, and lower reaches; and (3) quantify the dominant meteorological drivers of soil moisture under normal conditions and during typical extreme drought events using a generalized additive model. By clarifying the scale-dependent transition of soil moisture controls from precipitation supply to atmospheric evaporative demand, this study provides scientific support for improving drought early warning, agricultural drought assessment, and adaptive water resource management in the Yangtze River Basin.

2. Data and Methods

2.1. Study Area

The Yangtze River Basin (Figure 1) is located between 90°33′–122°25′ E and 24°30′–35°45′ N, covering a drainage area of approximately 1.8×10^6 km^2. The Yangtze River originates from the Qinghai–Tibet Plateau and flows eastward into the East China Sea, with a mainstream length of about 6300 km. The basin spans a pronounced west–east elevation gradient, ranging from high-altitude plateau and mountain regions in the upper reaches to hilly areas, basins, alluvial plains, and lake plains in the middle and lower reaches. The basin is mainly influenced by the East Asian monsoon climate, with marked seasonal and spatial differences in precipitation. Annual rainfall is concentrated mainly from June to August, and flood-season precipitation accounts for more than 60% of annual precipitation. Spatially, precipitation generally decreases from the humid southeastern and downstream regions toward the northwestern and upstream mountainous regions. In recent decades, under the combined influence of climate change and intensified human activities, the basin has experienced several regional and basin-wide drought events. For example, the extreme drought in 2022 caused substantial declines in tributary discharge and lake water levels, severely affecting navigation, agricultural irrigation, hydropower generation, and ecosystems [26]. The large differences in elevation, terrain, river network density, lake distribution, and climatic conditions among the upper, middle, and lower reaches make the Yangtze River Basin an appropriate region for investigating multiscale soil moisture dynamics and their meteorological controls.

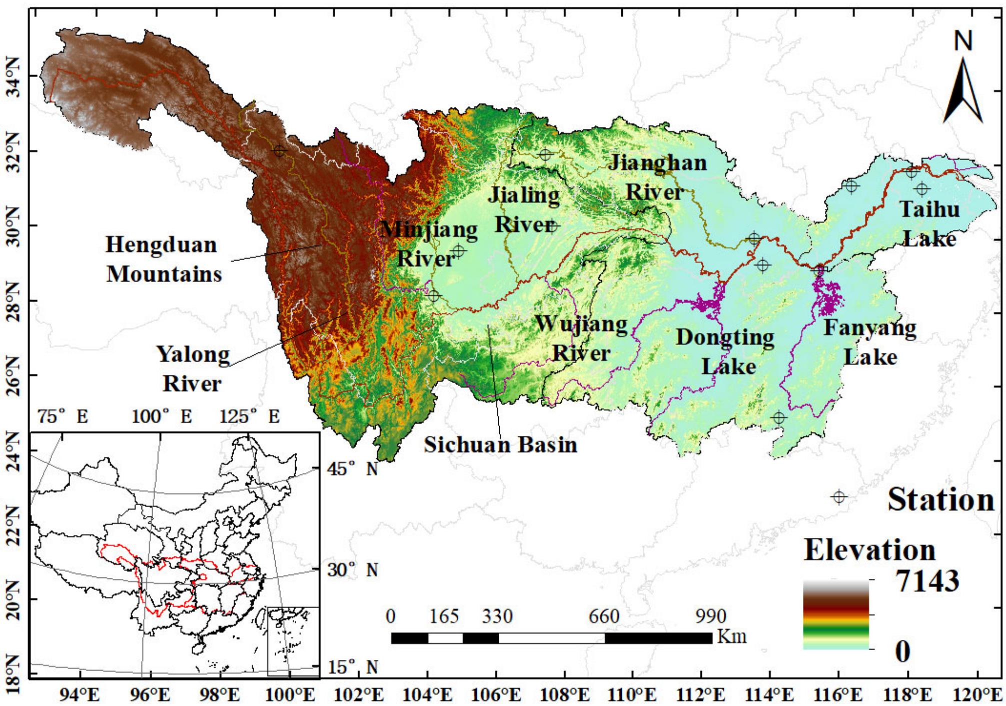

Figure 1. Yangtze River Basin.

2.2. Datasets

2.2.1. ESA CCI SM

Currently, numerous soil-water satellite products are available both domestically and internationally, including NASA's SMAP, the European Space Agency's SMOS, Japan's AMSR2, and China's Fengyun-3 series satellites (FY3B and FY3C). Previous validation studies have evaluated these products against in situ soil moisture observations, soil moisture monitoring networks, and land data assimilation or reanalysis products, using metrics such as correlation coefficient, bias, RMSE [28]. The soil moisture data employed in this study were obtained from the ESA Climate Change Initiative Soil Moisture combined product, which integrates active and passive microwave satellite retrievals into a long-term global surface soil moisture record, and were downloaded from the UK Centre for Environmental Data Analysis (CEDA) [15]. This dataset has a spatial resolution of 0.25° × 0.25° and a temporal resolution of 1 day, observing surface soil moisture (0–5 cm) from 1978 to the present (Table 1). As a widely used and longest time series remote-sensing soil moisture product globally, it has undergone extensive validation and provides substantial advantages over other products, including long time series, high stability, and comprehensive global coverage. The ESA CCI SM products primarily consist of three categories: active products from active microwave scatterometer measurements, passive products from passive microwave radiometer measurements, and integrated products that combine both types of microwave data. Integrated products maintain an optimal balance between temporal continuity and accuracy, making them the most commonly used and officially recommended product type [16]. This study used the V09.1 version of the CCI integrated product, covering the period from 1 January 2010, to 31 December 2022.

Table 1. Soil Moisture Products Introduction.

Soil Moisture Products	Depth	Time Resolution	Spatial Resolution	Source
ESACCI	0–5 cm	daily	0.25° × 0.25°	https://data.ceda.ac.uk accessed on 12 July 2025
ERA5	0–7 cm	daily	0.25° × 0.25°	https://cds.climate.copernicus.eu/api accessed on 12 July 2025
Site Data	0–10 cm	daily	point/station-based	https://data.cma.cn/ accessed on 12 July 2025

2.2.2. Validation Data

To evaluate the applicability of the ESA CCI SM product in the Yangtze River Basin, two independent reference datasets, listed in Table 1, were used for validation: ground-based observations and ERA5 reanalysis soil moisture. Ground observation data were obtained using the classical gravimetric method by measuring the soil moisture content at depths of 0–10 cm [29]. To account for Spatial disparities across the watershed, four representative stations were selected in each upstream, midstream, and downstream segment for validation (Table 2), which comprised major land-use types such as grasslands, farmland, and forests. In addition, ERA5 reanalysis data from the European Centre for Medium-Range Weather Forecasts were used as an auxiliary validation source. ERA5 soil moisture for the first soil layer (0–7 cm), obtained from the Climate Data Store, was compared with the ESA CCI SM product to provide an additional reference for evaluating its performance.

Table 2. Soil moisture Observation Stations Introduction.

Upper Reaches				Middle Reaches				Lower Reaches			
Site	Longitude (E°)	Latitude (N°)	Land Type	Site	Longitude (E°)	Latitude (N°)	Land Type	Site	Longitude (E°)	Latitude (N°)	Land Type
56,038	98.10	32.98	Grassland	57,128	107.33	33.17	Forest	58,510	116.23	29.73	Farmland
56,389	103.95	29.20	Farmland	57,494	114.05	30.60	Urban	58,321	117.30	31.78	Urban
56,295	104.55	30.38	Urban	57,590	114.37	29.85	Forest	58,252	119.47	32.18	Farmland
57,328	107.50	31.20	Forest	57,992	114.75	25.67	Farmland	58,342	119.55	31.72	Farmland

2.2.3. Meteorological Data

Considering data consistency and the occurrence of several representative drought events, the period from 2010 to 2022 was selected for the meteorological analysis. Although this period is shorter than the standard climatological reference period, this study focuses on recent soil moisture responses and driver mechanisms rather than long-term climate normals. The selected period covers typical drought events in the Yangtze River Basin and provides sufficient daily samples for weekly and monthly attribution analysis.

ERA5 soil moisture data were resampled to the same spatial resolution as ESA CCI, namely 0.25° × 0.25°, using bilinear interpolation. The monthly soil moisture values of the corresponding grid cells were then compared between the two products. For ground validation, each station was matched to the nearest ESA CCI grid cell according to its latitude and longitude using the nearest-neighbor method, and the corresponding soil moisture time series were compared. During the validation of ESACCI soil moisture data, multiple verification methods—including deviation, mean deviation, mean absolute deviation, and root mean square deviation—were employed to compare the results with ERA5 soil moisture data and ground-based soil moisture measurements, the results are presented below.

$$Bias_{\mathrm{i}} = \mathrm{y}_{\mathrm{sm,i}} - \mathrm{x}_{\mathrm{sm,i}} \tag{1}$$

$$Mean\_Bias = \frac{1}{N}\sum_{\mathrm{i}=1}^{N} Bias_{\mathrm{i}} \tag{2}$$

$$MAE = \frac{1}{\mathrm{n}}\sum_{\mathrm{i}=1}^{\mathrm{n}} \left| \mathrm{y}_{\mathrm{sm,\ i}} - \mathrm{x}_{\mathrm{sm,\ i}} \right| \tag{3}$$

$$RMSE_{\mathrm{i}} = \sqrt{\frac{1}{N}\left(ERA5_{\mathrm{sm,i}} - ESA_{\mathrm{sm,i}}\right)^2} \tag{4}$$

where $\mathrm{y}_{\mathrm{sm,i}}$ represents the monthly soil moisture values from ERA5 or ground-based observations, while $\mathrm{x}_{\mathrm{sm,i}}$ represents the monthly soil moisture values from ESA CCI.

The meteorological data used in this study comprised daily precipitation, temperature, wind speed, and saturated vapor pressure difference (VPD) from 2010 to 2022. Precipitation, temperature, and wind speed data were obtained from the National Meteorological Data Center, whereas VPD was calculated using the fifth-generation Global Reanalysis dataset (ERA5) released by the European Center for Medium-Range Weather Forecasts. Unlike precipitation, temperature, and wind speed, VPD is usually not directly measured, but derived from air temperature and humidity-related variables. In this study, ERA5 was used because it provides spatially continuous and temporally consistent temperature and humidity data across the Yangtze River Basin during the study period. Specifically, the 2 m dew point temperature and 2 m air temperature were extracted from the ERA5 dataset, and the saturated and actual vapor pressures were calculated using the Magnus–Tetens formula to obtain the VPD values [30].

The Magnus–Tetens formula is expressed as follows:

$$e_s = 0.6108 \times \exp\left(\frac{17.27 \times T}{T + 273.3}\right) \tag{5}$$

$$e_a = 0.6108 \times \exp\left(\frac{17.27 \times T_{dew}}{T_{dew} + 273.3}\right) \tag{6}$$

$$VPD = e_s - e_a \tag{7}$$

where VPD represents the saturated vapor pressure difference (kPa); es and ea represent the saturated vapor pressure and actual vapor pressure (kPa) at the current temperature, respectively; T is the temperature at a 2 m height (°C); and Tdew is the dew point temperature at a 2 m height (°C).

2.3. Dominant Factor Analysis Method

This study reconstructed daily soil moisture time series for the Yangtze River Basin from 2010 to 2022 using multi-source remote sensing data and conducted a systematic analysis of soil moisture dynamics across spatiotemporal dimensions. By integrating meteorological data, our study investigated the driving mechanisms of precipitation, temperature, wind speed, and VPD on soil moisture changes. To address the potential obscuring of long-term trends and the underlying effects of meteorological factors by seasonal fluctuations, seasonal adjustments were initially applied to both the soil moisture and meteorological variables to highlight their interannual variations and anomalous fluctuations. Subsequently, a Generalized Additive Model was employed to quantitatively identify the dominant factors influencing soil moisture dynamics, with the F-statistic used to assess the factor's relative contribution, thereby elucidating the key driving mechanisms of soil moisture changes.

The generalized additive model employs data-driven smoothing functions to overcome the limitations of linear assumptions. Its core advantages include the precise capture of highly nonlinear responses, high fitting accuracy, and distinct interpretable physical mechanisms that effectively mitigate collinearity interference. In this study, the GAM analysis was implemented in R to fit the nonlinear relationships between soil moisture and meteorological variables and to calculate the relative contribution of each factor [21]. The formula used is expressed as follows:

$$y(SM_i) = \beta + s(T_i) + s(W_i) + s(VPD_i) + s(P_i) + \in \tag{8}$$

where SM_i represents soil moisture, T_i represents temperature (°C), W_i indicates wind speed (m/s), VPD_i is the vapor pressure difference (kPa), and P_i represents precipitation (mm). The same smoothing basis dimension was used for all meteorological variables in the main model to ensure comparability among the smooth terms. The individual effect of each variable was evaluated using the F-statistic of its smoothing term. The relative importance of each factor was calculated as

$$RCi = Fi/\sum Fi \times 100\% \tag{9}$$

where Fi is the F-statistic of the smoothing term for factor i, and RCi represents the GAM-derived relative contribution of factor i. In this study, the dominant meteorological factor at each grid cell was defined as the variable with the largest F-statistic, indicating the strongest individual association with soil moisture variability within the GAM framework. Basin-scale and regional RC values were obtained by averaging the grid-cell RC values across all valid grid cells. To avoid overstating the precision of single percentage values, the mean F-statistic, mean RC, and 95% confidence intervals of the spatial mean RC were also calculated.

To examine the robustness of the GAM results, several sensitivity tests were conducted. First, alternative smoothing basis dimensions were tested to assess whether the estimated individual effects were sensitive to the choice of smoothing parameters [23]. Second, different smoothing parameter selection methods, including REML, ML, and GCV.Cp, were compared. Third, concurvity diagnostics were used to examine nonlinear dependence among explanatory variables, and models excluding temperature, VPD, or wind speed were fitted separately to evaluate the influence of potentially collinear variables. Fourth, the results based on deseasonalized anomalies were compared with those obtained from the original non-deseasonalized data to assess the effect of the seasonal adjustment step. Finally, an alternative model including a VPD-precipitation interaction term was tested. These sensitivity analyses were used to evaluate whether the identified dominant factors and relative importance rankings were stable under different model settings.

3. Results

3.1. Evaluation of ESA CCI SM

This study evaluated ESA CCI soil moisture against observations from four field stations in the upper, middle, and lower reaches of the Yangtze River Basin during 2010–2013 (Figure 2a,b). The mean absolute deviations were 0.0460, 0.0434, and 0.0072 m^3/m^3 in the upper, middle, and lower reaches, respectively. The largest deviations occurred in the upper reaches, where rugged terrain and strong surface heterogeneity can reduce the representativeness of satellite pixels. The middle reaches also showed large station-to-station variations, probably related to heterogeneous land cover and vegetation conditions. In contrast, the lower reaches had the smallest deviation, reflecting the relatively flat terrain and more homogeneous surface conditions. Taylor plots showed that correlation coefficients were mostly between 0.4 and 0.7. These moderate correlations are reasonable because field measurements represent local soil moisture conditions, whereas ESA CCI pixels represent area-averaged values. Overall, ESA CCI soil moisture captured the temporal variation in field-observed soil moisture and was suitable for regional-scale temporal analysis (Figure 2c).

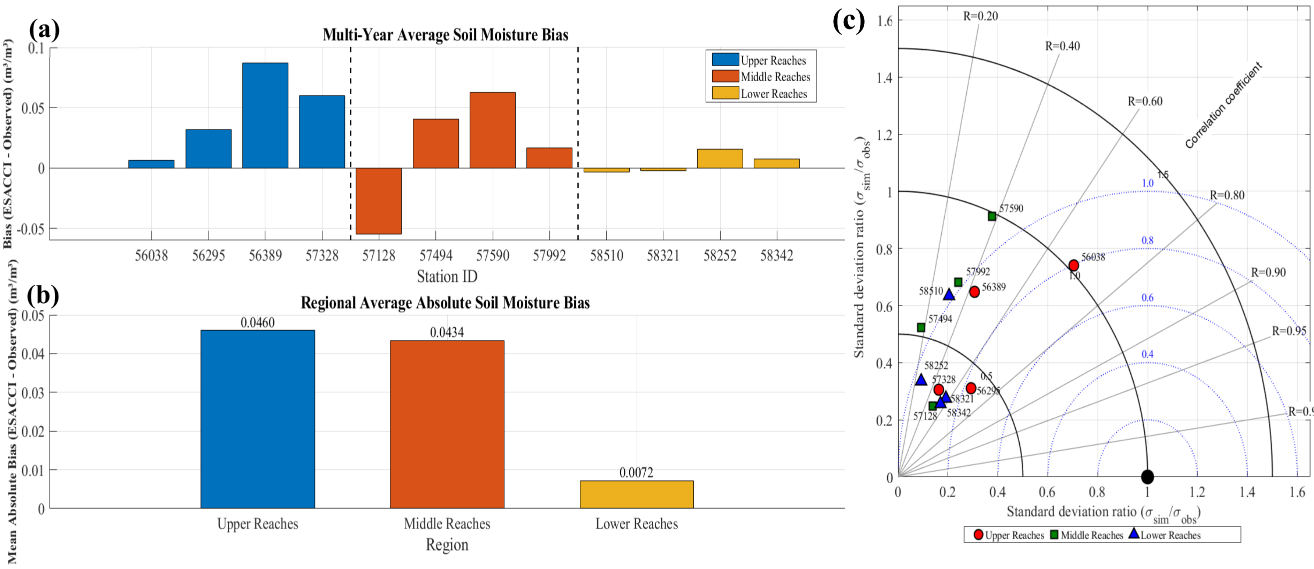

Figure 2. Comparison between CCI and measured station data. (**a**) Muti-year average soil moisture bias; (**b**) regional average absolute soil moisture bias; (**c**) Taylor diagram.

The comparison with ERA5 further confirmed the spatial reliability of ESA CCI soil moisture (Figure 3a,b). The basin-mean RMSE was 0.0127 m^3/m^3, indicating small differences between the two products. Low RMSE values dominated most areas of the basin, suggesting consistent temporal fluctuations between ESA CCI and ERA5. Higher RMSE values were mainly distributed along mountain margins and transitional zones in the northern and northwestern basin, where complex terrain increases retrieval uncertainty [31,32]. The basin-mean bias was -0.0079 m^3/m^3, and most areas showed near-zero bias, indicating good agreement in long-term mean soil moisture. Local positive or negative biases occurred in parts of the central, northern, and southwestern basin. These deviations may be associated with complex topography, seasonal freezing or snow cover, high-altitude hydrothermal processes, and dense vegetation, which can reduce microwave sensitivity to surface soil moisture. Overall, the low RMSE and near-zero mean bias indicate that ESA CCI soil moisture effectively captures basin-scale spatiotemporal variability and can support subsequent multiscale analysis.

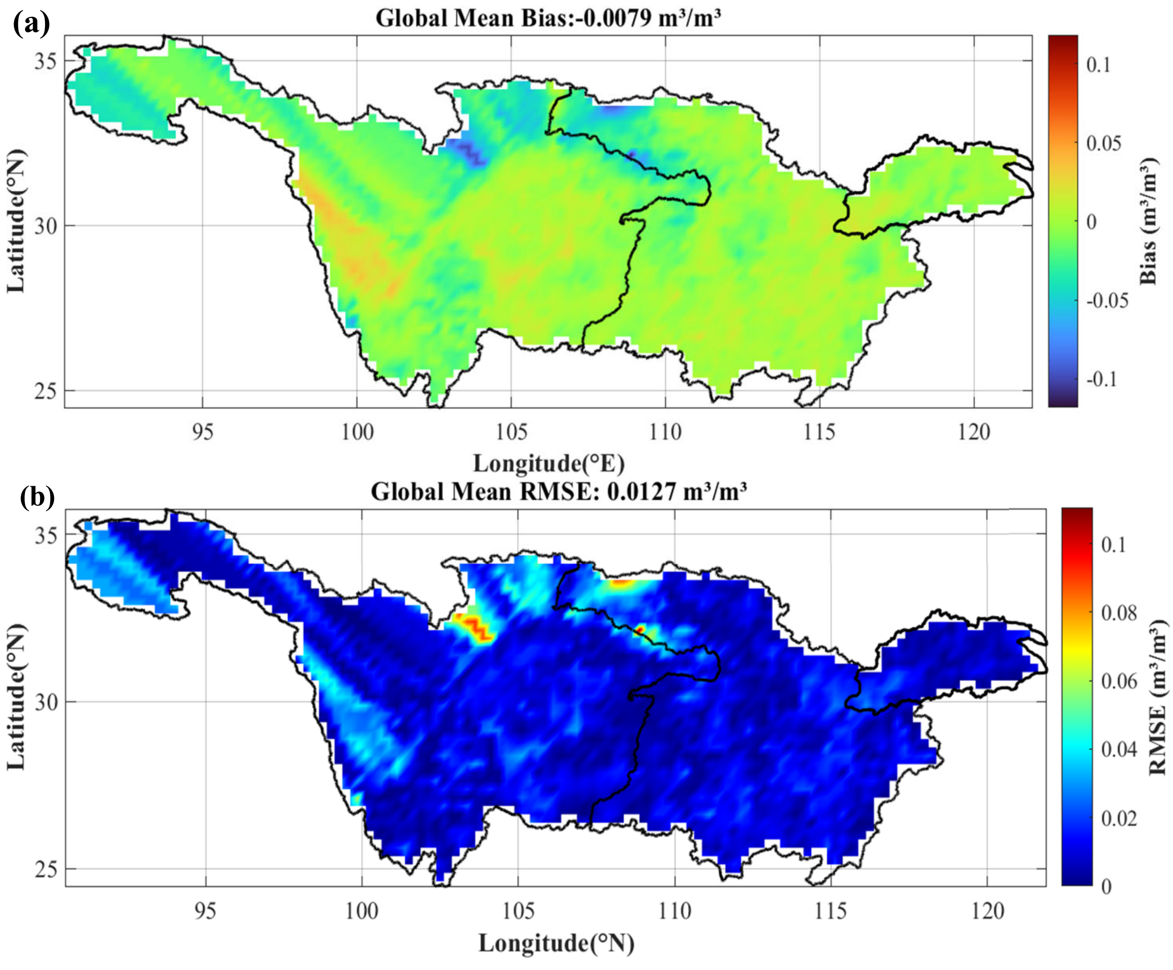

Figure 3. Comparison of (**a**) deviations unbiased and (**b**) mean square error between ERA5 and ESACCI products.

3.2. Spatiotemporal Change Analysis

3.2.1. Temporal Variation

Figure 4a shows the temporal variation in ESA CCI soil moisture across the Yangtze River Basin from 2010 to 2022 at weekly, monthly, and annual scales.

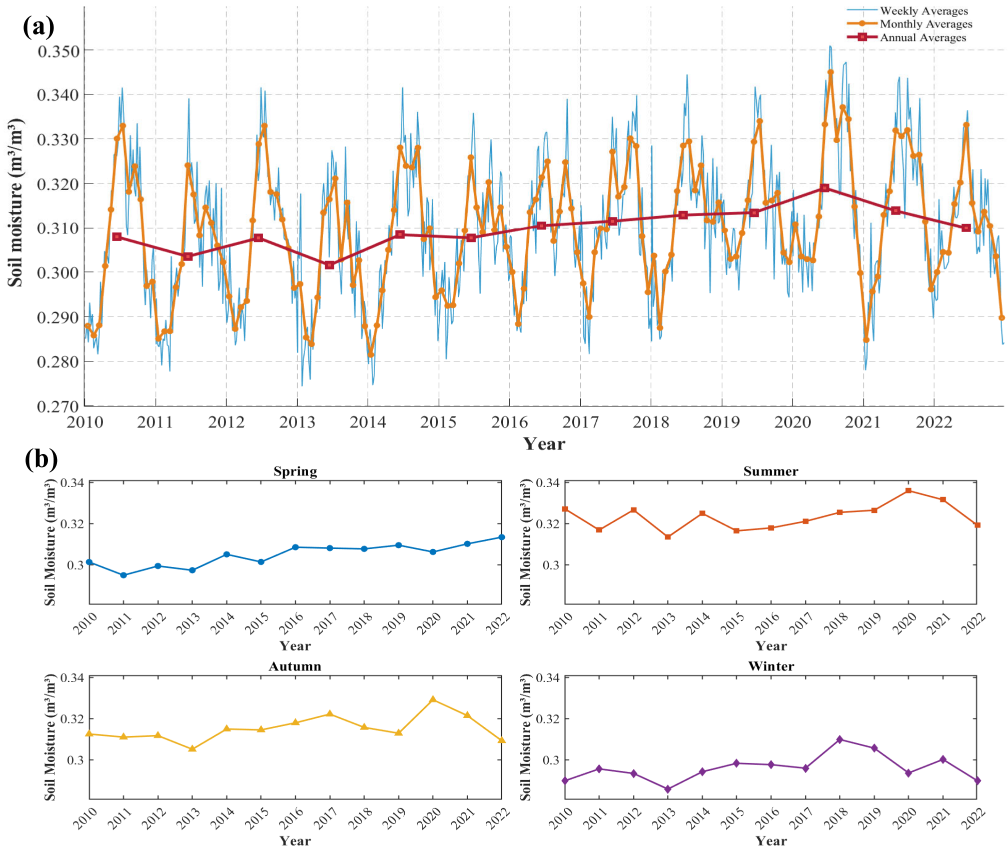

Figure 4. Changes in soil moisture at different (**a**) temporal scales and (**b**) seasonal scales.

At the weekly scale, soil moisture showed the largest fluctuation range (Figure 4a). This reflects the rapid response of surface soil moisture to short-term precipitation infiltration, evapotranspiration, and temperature changes [33]. Weekly data also captured more frequent peak and trough values, which may correspond to extremely wet or dry weeks. At the monthly scale, high-frequency weekly fluctuations were smoothed, but the seasonal cycle remained clear. Both weekly and monthly series showed a consistent wet–dry alternation, with soil moisture generally increasing during the wet season and decreasing during the dry season. The overall fluctuation range was approximately 0.28–0.35 m^3/m^3, indicating strong sensitivity of soil moisture to seasonal hydrothermal conditions in the Yangtze River Basin. Compared with monthly averages, weekly data better represented short-term hydrological processes, including precipitation, runoff, and evapotranspiration.

At the annual scale, soil moisture showed clear phase-specific changes (Figure 4a). From 2010 to 2013, annual mean soil moisture decreased slightly from approximately 0.308 to 0.302 m^3/m^3, indicating a relatively dry phase. From 2014 to 2020, soil moisture increased steadily and reached approximately 0.319 m^3/m^3 in 2020, suggesting improved basin-scale water availability. From 2021 to 2022, soil moisture decreased to approximately 0.310 m^3/m^3, indicating a shift toward drier conditions and stronger water loss. These interannual variations may reflect the combined effects of regional climate variability, land-surface conditions, and human activities. Seasonal variations also showed a clear pattern (Figure 4b). Soil moisture generally increased in spring due to rainfall recharge, reached its highest level in summer, and then declined from autumn to winter.

Overall, ESA CCI soil moisture showed significant seasonal cycles at weekly and monthly scales in the Yangtze River Basin. Weekly soil moisture was more sensitive to short-term meteorological and hydrological fluctuations, whereas monthly averages retained the main intra-annual wet–dry transitions after smoothing high-frequency variability. The annual series further revealed distinct interannual changes, indicating the influence of longer-term climatic and hydrological conditions on basin-scale soil moisture [33].

3.2.2. Spatial Variation

Owing to the extensive coverage of the study area and notable variations in meteorological conditions and surface elements across different regions, this study further analyzed the spatial distribution of soil moisture in the upper, middle, and lower reaches of the Yangtze River Basin (Figure 5a).

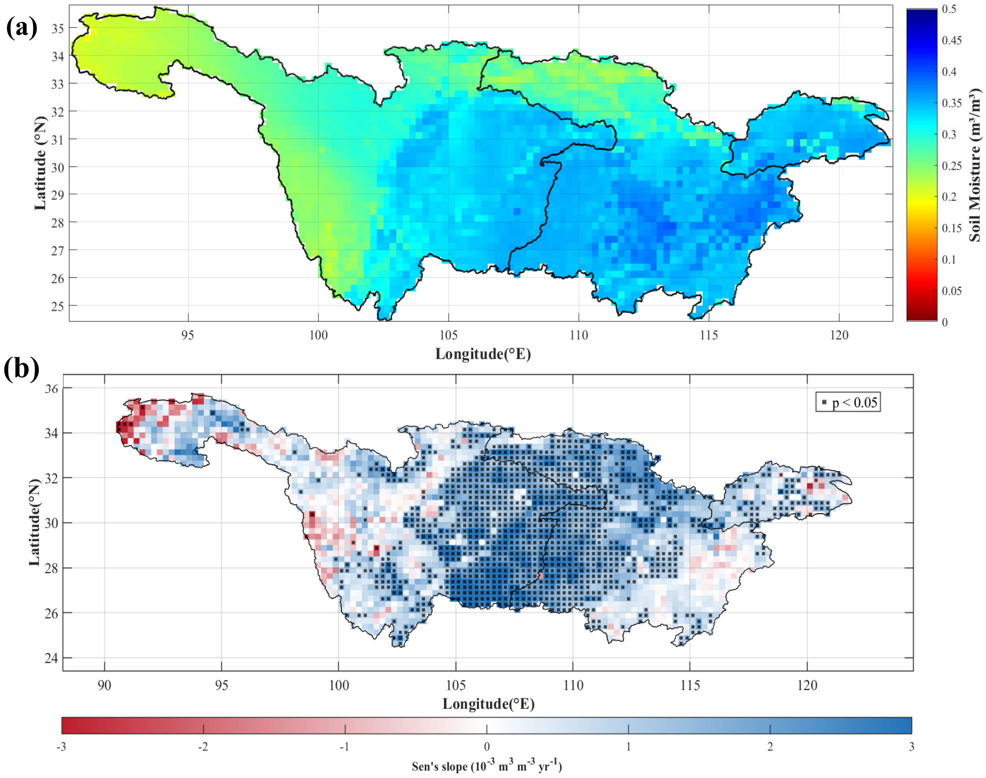

Figure 5. Spatial distribution of (**a**) soil moisture and (**b**) trend changes.

In the upper reaches, soil moisture showed strong Spatial disparities and a clear west–east gradient [10]. Lower values were mainly distributed in the western and northwestern regions, whereas higher values occurred in the eastern and southeastern regions. Soil moisture was generally within 0.20–0.35 m^3/m^3. This pattern is closely related to rugged terrain, high elevation, and steep slopes. These conditions promote rapid runoff generation and reduce soil moisture infiltration. Thin soil layers and uneven precipitation further enhance Spatial disparities. Thus, soil moisture in the upper reaches is mainly controlled by terrain and local hydrological processes.

In the middle reaches, soil moisture was higher and more spatially continuous than in the upper reaches. Most areas showed medium-to-high values of 0.30–0.45 m^3/m^3, forming a broad zone of relatively high soil moisture. Only small low-value patches appeared in the northern part. The reduced Spatial disparities is associated with flatter terrain, greater precipitation, and a dense network of rivers, lakes, and wetlands. These conditions enhance surface water–groundwater exchange and support soil moisture storage. In addition, soils with stronger water-holding capacity favor the accumulation and maintenance of soil moisture.

In the lower reaches, soil moisture was relatively uniform and mainly ranged from 0.35 to 0.45 m^3/m^3. Most areas maintained high soil moisture, with limited spatial variation. This reflects the influence of low-lying terrain, shallow groundwater, and abundant precipitation, which together maintain a humid soil hydrological environment. Intensive agriculture and irrigation may further increase baseline soil moisture and reduce local variability.

Figure 5b further shows the spatial trend of soil moisture in the Yangtze River Basin. Decreasing trends were mainly observed in parts of the upper reaches, indicating that these high-altitude and mountainous areas may be more sensitive to soil moisture loss and drought stress [5]. In contrast, increasing trends appeared in parts of the middle reaches, suggesting improved soil moisture availability and a stronger capacity to buffer drought impacts. The lower reaches showed relatively weak trends and smaller spatial differences, indicating more stable soil moisture conditions in lowland and lake-plain areas. Overall, the trend pattern reveals clear spatial differentiation in soil moisture change, with greater vulnerability in parts of the upper reaches and relatively stronger drought-buffering conditions in parts of the middle and lower reaches.

3.3. Dominant Factors Analysis

3.3.1. Analysis of Soil Moisture Driving Factors at Different Time Scales

The preceding analysis showed clear multiscale spatiotemporal variations in soil moisture across the Yangtze River Basin. To identify the meteorological controls at different temporal scales, this study selected precipitation, temperature, wind speed, and VPD as explanatory variables. A generalized additive model was used to quantify their relative contributions at weekly and monthly scales.

At the weekly scale, VPD was the dominant factor controlling soil moisture variability in the Yangtze River Basin (Figure 6). Its mean relative contribution reached 47.04%, and its dominant areas were widely distributed across the basin, especially in the upper and lower reaches. This pattern indicates that short-term soil moisture changes were mainly associated with VPD. Precipitation showed the second-largest mean relative contribution, accounting for 24.38%, followed by temperature at 18.02%. Their dominant areas were more scattered, suggesting that short-term rainfall inputs and thermal conditions affected soil moisture in a more localized manner. Wind speed had the lowest mean relative contribution, accounting for 10.55%, and was mainly distributed in limited parts of the basin. This indicates a weaker but still observable effect of wind-driven turbulent exchange on surface soil moisture loss. Overall, the weekly-scale results show that soil moisture variability was primarily related to VPD, while precipitation, temperature, and wind speed played secondary and spatially heterogeneous roles.

At the weekly scale, VPD had the strongest GAM individual effect on soil moisture, followed by precipitation, temperature, and wind speed. The 95% confidence intervals showed that this ranking was relatively stable at the basin scale, supporting the dominant role of atmospheric evaporative demand in short-term soil moisture variability (Table 3).

Table 3. Weekly-scale GAM F-statistic table for the Yangtze River Basin.

Factor	Mean F-Statistic	Relative Importance (%)	95% CI (%)
Precipitation	14.40	24.38	23.74–25.03
VPD	30.91	47.04	46.28–47.80
Temperature	17.96	18.02	17.34–18.70
Wind speed	7.60	10.55	10.11–11.00

At the monthly scale, the dominant controls changed markedly (Figure 7). Precipitation became the primary dominant factor, with the highest mean relative contribution of 36.62%. Its dominant areas were mainly distributed in the upper and middle reaches, indicating that accumulated precipitation and infiltration played a major role in regulating monthly soil moisture variability. VPD showed the second-largest mean relative contribution, accounting for 26.58%, and was distributed across parts of the upper and middle reaches, suggesting that atmospheric evaporative demand still affected monthly soil moisture conditions. Temperature accounted for 22.49%, with dominant areas mainly in the middle and lower reaches, reflecting the role of thermal conditions in monthly soil moisture balance. Wind speed had the lowest mean relative contribution, accounting for 14.31%, and showed a relatively scattered distribution. Overall, monthly soil moisture was mainly associated with precipitation supply, while VPD, temperature, and wind speed exerted secondary.

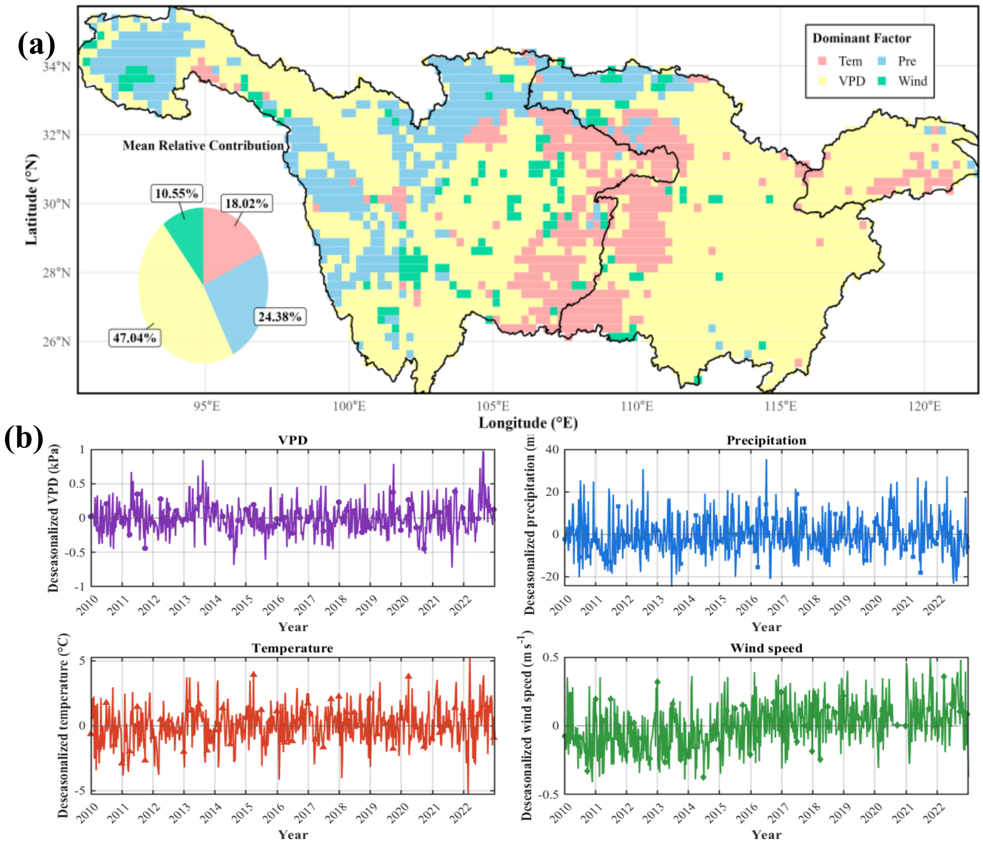

Figure 6. Relative contributions of meteorological factors at the weekly scale. (**a**) Spatial patterns; (**b**) Temporal patterns.

The results indicate that precipitation had the strongest monthly-scale individual effect on soil moisture, followed by VPD, temperature, and wind speed. The 95% confidence intervals further indicate that the ranking of the main meteorological controls was relatively stable at the basin scale (Table 4).

Table 4. Monthly-scale GAM F-statistic table for the Yangtze River Basin.

Factor	Mean F-Statistic	Relative Importance (%)	95% CI (%)
Precipitation	4.48	36.62	35.63–37.62
VPD	3.98	26.58	25.83–27.32
Temperature	3.46	22.49	21.83–23.15
Wind speed	1.93	14.31	13.72–14.90

https://doi.org/10.3390/atmos17080781

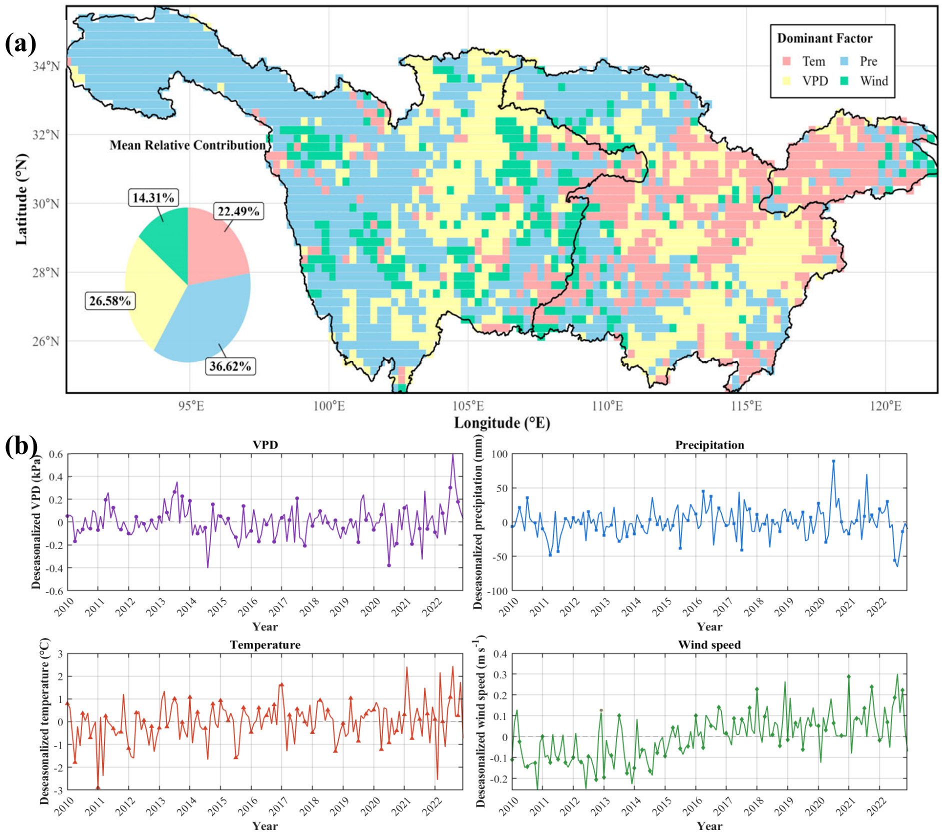

Figure 7. Relative contributions of meteorological factors at the Monthly scale. (**a**) Spatial patterns; (**b**) Temporal patterns.

3.3.2. Analysis of Driving Factors of Drought Events

Recently, drought events have occurred frequently in the Yangtze River Basin, underscoring the important role of soil moisture in drought impacts. The three typical drought events were selected based on the Standardized Precipitation Evapotranspiration Index (SPEI) and their spatial extent within the Yangtze River Basin. Drought periods were identified when SPEI indicated drought conditions over a large proportion of the basin, representing large-scale drought episodes within the basin, and were suitable for comparing soil moisture responses and dominant meteorological controls during drought conditions. Therefore, this study selected three typical drought events (2011, 2019, and 2022) to further investigate the changes in soil moisture during droughts and their driving factors.

Figure 8 shows the zonal variations in soil moisture during the three drought events. At the weekly scale, soil moisture anomalies were more spatially fragmented than at the monthly scale. This reflects the stronger influence of short-term hydrological processes. In Event 1, the broad monthly drought areas were separated into smaller weekly drought patches. In Event 2, soil moisture deficits remained concentrated in the middle and lower reaches at both monthly and weekly scales. This suggests a persistent drought signal during this event. In Event 3, the weekly results showed a stronger drought signal in the upper reaches than the monthly results. This difference may be related to intermittent precipitation, which can partly reduce monthly drought intensity.

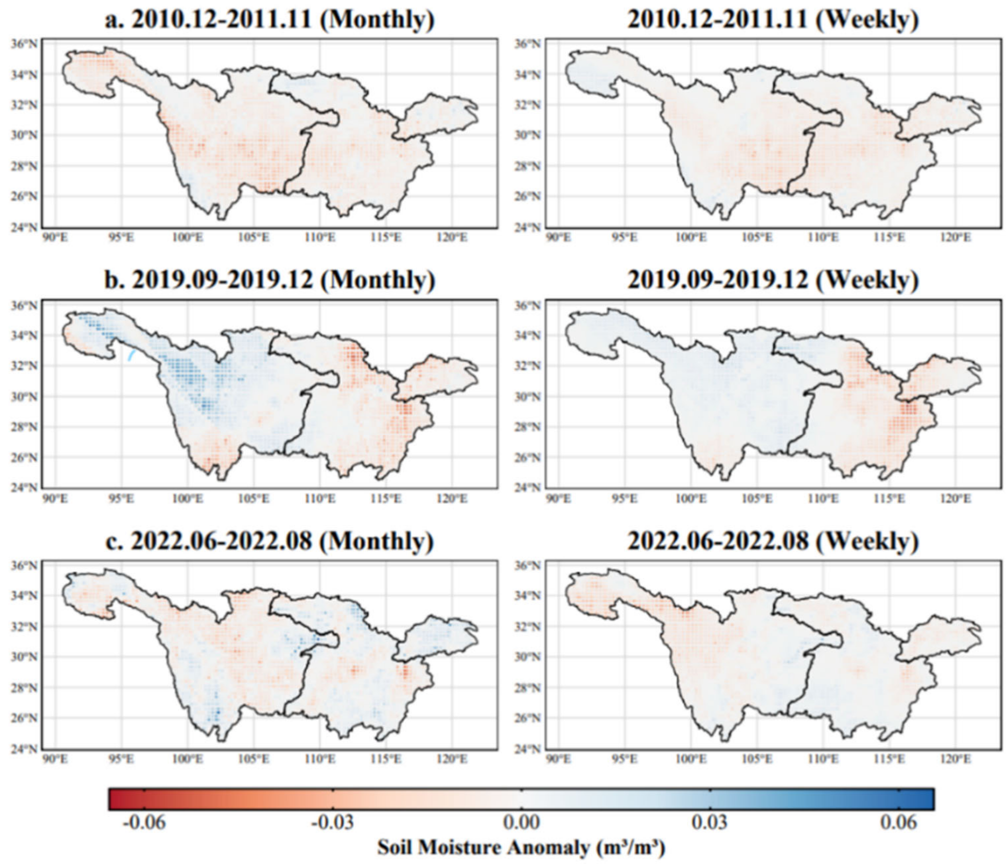

Figure 8. Soil moisture anomaly variations during drought periods. (**a**) 2010.12–2011.11; (**b**) 2019.09–2019.12; (**c**) 2022.06–2022.08.

At the monthly scale, the events showed different spatial patterns and drought intensities. Event 1 (December 2010–November 2011) showed widespread negative anomalies in the middle and lower Yangtze River Basin, ranging from -0.04 to -0.06 m^3/m^3 (Figure 8a). The drought mainly affected the central and eastern parts of the basin. Event 2 (September 2019–December 2019) showed the strongest spatial contrast (Figure 8b). Severe soil moisture deficits occurred in the lower reaches, with anomalies close to -0.06 m^3/m^3, whereas positive anomalies of approximately +0.06 m^3/m^3 appeared in parts of the middle and upper reaches. This formed a clear east–west dry–wet contrast. Event 3 (June 2022–August 2022) showed alternating dry and wet patterns (Figure 8c). Moderate soil moisture deficits of -0.02 to -0.04 m^3/m^3 occurred in parts of the middle and lower reaches, while localized wet areas were also observed. This indicates strong Spatial disparities in basin water conditions.

Soil moisture integrates the effects of precipitation, evaporation, transpiration, and runoff. The three drought events showed distinct spatiotemporal patterns, indicating that their formation mechanisms were not identical. Therefore, the dominant meteorological factors during drought periods were further analyzed to identify the controls on soil moisture evolution (Figure 9).

At the weekly scale, the dominant pattern was clearer (Figure 8). VPD had the largest GAM-derived relative contribution in all three drought events, accounting for 44.12%, 42.19%, and 36.20% in 2010.12–2011.11, 2019.09–2019.12, and 2022.06–2022.08, respectively. Its dominant areas also showed stronger spatial continuity than those of the other factors. Precipitation ranked second, with contributions of 25.62%, 27.24%, and 30.21%, indicating that short-term rainfall anomalies still affected soil moisture during drought periods. Temperature contributed 19.81%, 16.92%, and 18.19%, whereas wind speed contributed 10.45%, 13.65%, and 15.40%. Overall, the weekly-scale results suggest that rapid soil moisture depletion during drought events was mainly associated with atmospheric evaporative demand, while precipitation, temperature, and wind speed played secondary but event-dependent roles.

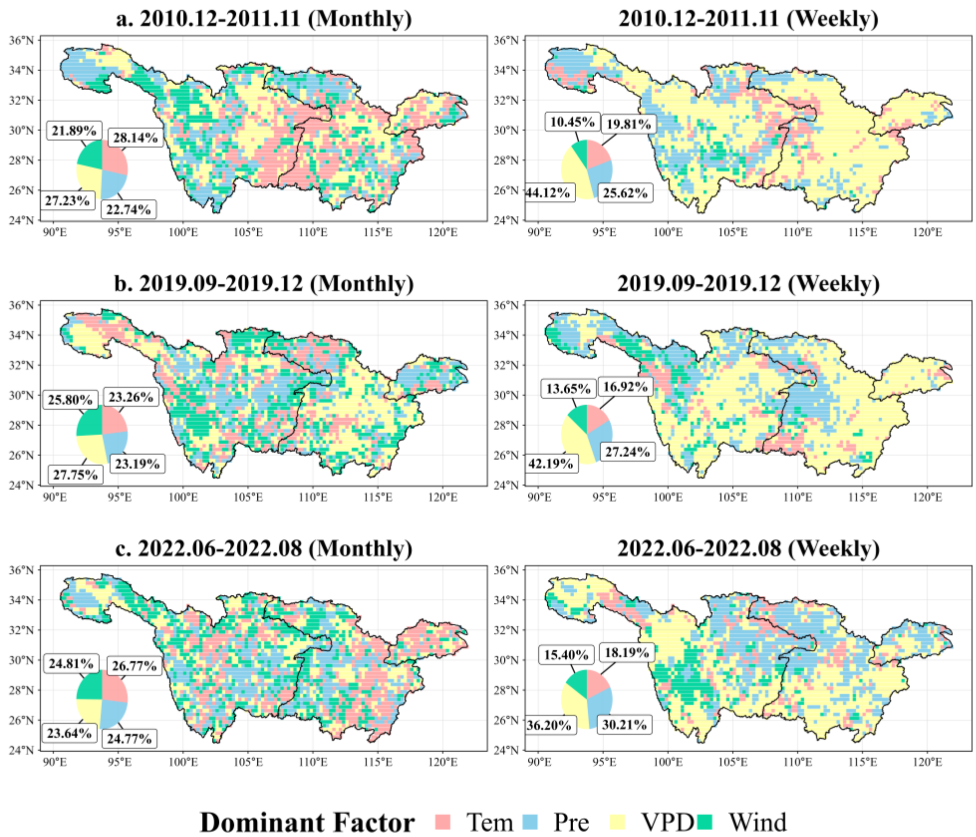

Figure 9. Relative contributions of meteorological factors during drought periods. (**a**) 2010.12–2011.11; (**b**) 2019.09–2019.12; (**c**) 2022.06–2022.08.

At the monthly scale, no single meteorological factor consistently dominated soil moisture changes during drought events (Figure 8). The GAM-derived relative contributions of precipitation, temperature, VPD, and wind speed were relatively close. In the 2010.12–2011.11 event, temperature and VPD contributed 28.14% and 27.23%, respectively, while precipitation and wind speed contributed 22.74% and 21.89%. In the 2019.09–2019.12 event, VPD showed the highest contribution at 27.75%, followed by wind speed, temperature, and precipitation, with values of 25.80%, 23.26%, and 23.19%, respectively. In the 2022.06–2022.08 event, temperature contributed the most, 26.77%, but precipitation, wind speed, and VPD also remained comparable, contributing 24.77%, 24.81%, and 23.64%, respectively. These results indicate that monthly soil moisture anomalies during drought events were jointly regulated by water supply, atmospheric dryness, thermal conditions, and turbulent exchange, rather than by a single meteorological factor [34,35].

4. Discussion

4.1. Analysis of Variability in Dominant Soil Moisture Factors Across Different Dimensions

The soil moisture controls showed a clear temporal shift (Figure 10). At the weekly scale, VPD was the dominant associated factor in the upper, middle, and lower reaches, contributing 42.51%, 52.15%, and 55.92%, respectively. This agrees with previous studies showing that atmospheric evaporative demand is closely linked to rapid surface soil drying. Fu et al. (2022) found that VPD can suppress ecosystem water exchange across a wide range of soil moisture conditions, while Gamelin et al. (2022) showed that VPD is an effective indicator of short-term drought extremes [36,37]. These findings support our result that VPD had the strongest weekly-scale association with rapid soil moisture decline. Precipitation played a secondary weekly role, especially in the upper reaches, with a contribution of 29.02%, but its contribution declined to 19.16% and 15.26% in the middle and lower reaches. At the monthly scale, precipitation became dominant in the upper reaches, contributing 44.69%, reflecting cumulative rainfall recharge. In the middle reaches, VPD, temperature, and precipitation had comparable contributions, 31.18%, 29.63%, and 27.29%, respectively. In the lower reaches, temperature showed the highest contribution, 42.74%, suggesting the importance of atmospheric energy conditions in humid lowland areas. Compared with previous studies that often examined a single time scale, our results show that soil moisture regulation shifts from short-term atmospheric-demand control at the weekly scale to more region-specific controls at the monthly scale, including precipitation supply in the upper reaches, mixed atmospheric and rainfall effects in the middle reaches, and temperature control in the lower reaches.

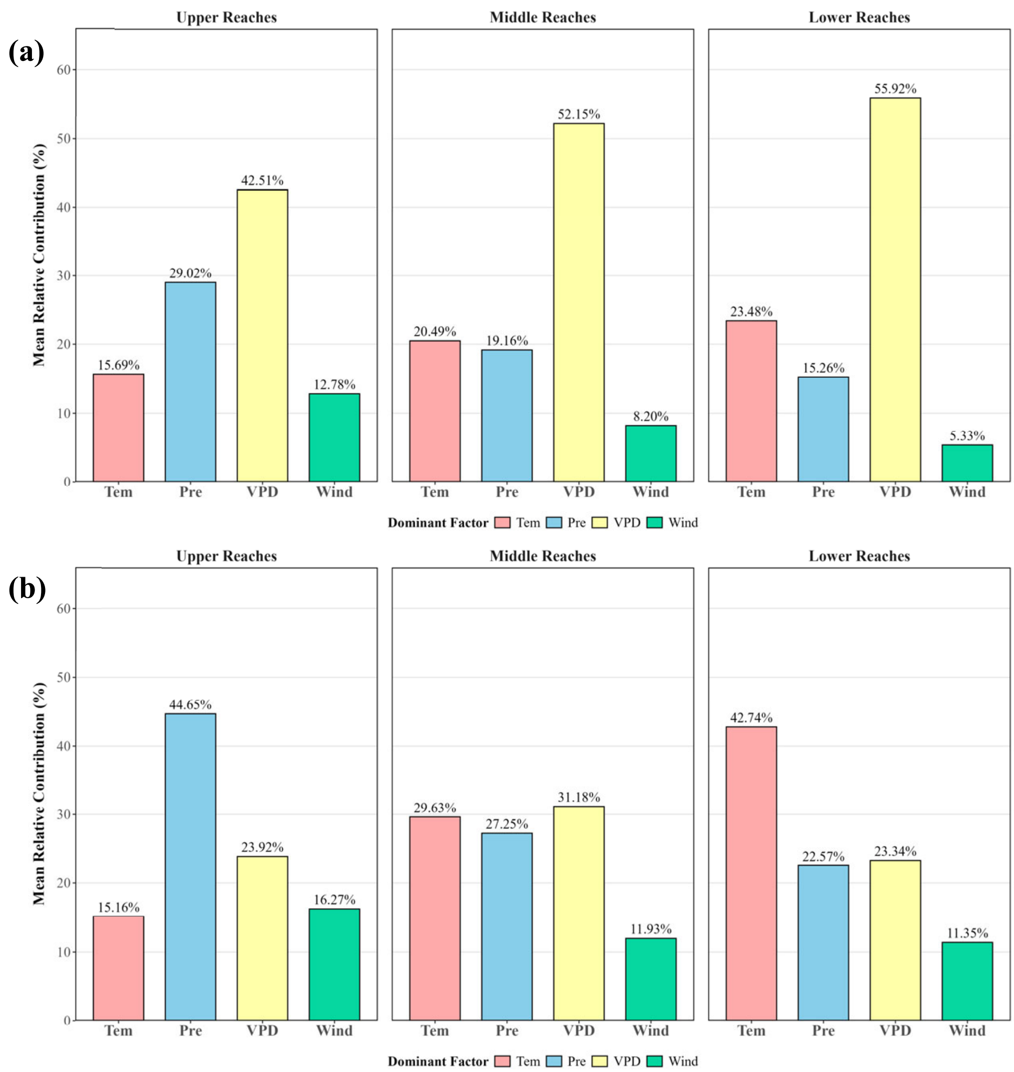

Figure 10. Spatial distribution of the relative contributions of meteorological factors to soil moisture variation at the (**a**) weekly and (**b**) monthly scales.

Spatially, the GAM-derived mean relative contributions showed a clear upstream–downstream transition. At the monthly scale (Figure 10b), precipitation was the main factor in the upper reaches, contributing 44.65%, followed by VPD, wind speed, and temperature, with contributions of 23.92%, 16.27%, and 15.16%, respectively. This indicates that soil moisture in the high-altitude and topographically complex upper basin remains strongly dependent on accumulated rainfall recharge, consistent with previous studies showing that terrain and local hydroclimatic conditions strongly regulate soil moisture in mountainous regions [32]. In the middle reaches, VPD, temperature, and precipitation contributed 31.18%, 29.63%, and 27.25%, respectively, suggesting a transitional regime jointly regulated by water supply and atmospheric demand. In the lower reaches, temperature showed the highest monthly contribution, 42.74%, whereas VPD and precipitation contributed 23.34% and 22.57%, respectively, indicating that thermal conditions become more important in regulating monthly soil moisture balance in humid lowland areas.

At the weekly scale (Figure 10a), VPD was the dominant factor in all three reaches. Its contribution increased from 42.51% in the upper reaches to 52.15% in the middle reaches and 55.92% in the lower reaches. Precipitation contributed 29.02% in the upper reaches but declined to 19.16% and 15.26% in the middle and lower reaches, respectively. This pattern indicates that short-term soil moisture variation is more sensitive to atmospheric evaporative demand than to rainfall input, especially in the middle and lower reaches. Temperature and wind speed played secondary roles, but their contributions varied regionally. Overall, from upstream to downstream, the dominant mechanism regulating soil moisture in the Yangtze River Basin exhibits a spatial evolution pattern shifting from precipitation replenishment and multifactor coupling control to atmospheric evapotranspiration demand dominance.

4.2. Analysis of Variability Between Multiyear Averages and the Dominant Soil Moisture Factors During Drought Events

At the weekly scale, VPD dominated soil moisture changes under both normal and drought conditions. During the three drought events, its contribution remained above 35%, clearly exceeding those of precipitation, temperature, and wind speed. This supports previous findings that atmospheric dryness can rapidly intensify surface soil moisture loss during short dry periods [31]. In contrast, precipitation had a consistently low contribution, suggesting that intermittent rainfall is less effective in regulating weekly soil moisture. Thus, weekly soil moisture analysis should give particular attention to VPD and atmospheric evaporative demand.

At the monthly scale, the dominant mechanism changed markedly. Under normal conditions, precipitation was the main driver, contributing 36.62%, which confirms the importance of accumulated rainfall recharge for monthly soil moisture storage. During drought events, however, precipitation dominance weakened, and the four meteorological factors contributed more evenly, generally within 20–30%. This is consistent with studies showing that drought development reflects the combined effects of precipitation deficit, high temperature, enhanced atmospheric demand, and turbulent water loss. Compared with previous studies that often emphasized precipitation deficits, our results show that monthly drought-related soil moisture changes should be interpreted as a coupled supply–demand process rather than a single-factor response.

4.3. Limitations

This study comprehensively analyzed the evolutionary patterns of soil moisture in the Yangtze River Basin across multiple spatiotemporal scales, including years, months, weeks, and upstream, midstream, and lower reaches. Using a GAM, we quantified the mechanisms underlying the influence of meteorological drivers and revealed how extreme drought events alter the spatial distribution of dominant factors. Several limitations remain in this study. The 0.25° ESA CCI soil moisture product is suitable for basin-scale analysis, but it cannot fully capture local heterogeneity caused by micro-topography, land cover differences, and local climate conditions. Uncertainty may also arise from the different representative depths of the validation datasets. Ground observations were measured at 0–10 cm, ESA CCI SM mainly represents approximately 0–5 cm, and ERA5 represents the first soil layer of 0–7 cm. Although these datasets all describe near-surface soil moisture, the depth mismatch may affect validation results, especially after rainfall when vertical soil moisture gradients are strong. No depth conversion was applied because vertically resolved observations were unavailable and the compared layers are relatively close in depth. In addition, soil moisture memory may influence the apparent contribution of meteorological factors. Deseasonalization reduced the effect of regular seasonal cycles, but it could not fully remove persistence caused by antecedent wetness, previous precipitation, vegetation, soil texture, and hydrological storage. Therefore, the GAM results should be interpreted as contemporaneous associations rather than explicit estimates of lagged effects. Satellite products mainly represent surface soil moisture and provide limited information on root-zone and deep-layer water. Human activities, including reservoir regulation, irrigation, land-use change, and vegetation restoration, were also not fully separated from meteorological forcing.

Future research should use higher-resolution and multi-source soil moisture products to improve the representation of local spatial variability. Vertically resolved soil moisture observations or model simulations are needed to characterize root-zone and deep-layer soil water. Human impacts should be examined separately from climatic forcing in highly managed basins. Longer observational records, coupled hydrological models, and data-driven methods would further improve the evaluation of soil moisture responses and the prediction of drought-related soil moisture deficits in large river basins.

5. Conclusions

This study used the ESA CCI soil moisture product, together with ground observations and ERA5 reanalysis data, to evaluate its applicability in the Yangtze River Basin through multiscale accuracy assessments. The validation results indicate that ESA CCI SM can generally capture basin-scale soil moisture variation, but its performance differs among regions. The product showed better agreement in the lower reaches, whereas larger deviations were observed in the upper and middle reaches. Based on this applicability assessment, we further examined soil moisture dynamics at weekly and monthly scales and analyzed the relative contributions of precipitation, temperature, VPD, and wind speed. The driving-factor analysis was conducted under both normal conditions and typical drought events to explore whether the dominant controls of soil moisture changed during drought periods. The key findings include:

(1) Comparative analysis between ground observations and ESA CCI soil moisture data showed that the accuracy of ESA CCI varied across different regions. Among the three subregions, ESA CCI showed the best agreement with ground observations in the lower reaches, followed by the middle and upper reaches. The average absolute deviations from upstream to downstream were 0.0460, 0.0434, and 0.0072 m^3/m^3, respectively. When compared with the ERA5 product, the global average deviation was -0.0079 m^3/m^3, and the root mean square error was 0.0127 m^3/m^3. These results indicate that the ESA CCI soil moisture product demonstrates good applicability across the Yangtze River Basin and effectively represents regional-scale soil moisture variation.

(2) The ESA CCI SM results indicated that soil moisture in the Yangtze River Basin exhibits significant seasonal and interannual variations over time. The patterns of soil moisture change differed notably across the different timescales; weekly fluctuations were pronounced, whereas monthly and annual variations were relatively smooth. This indicates that soil moisture effectively characterizes the transition between dry and wet conditions in the study area and captures changes during extreme meteorological and

hydrological events. Spatially, soil moisture showed a gradually increasing distribution pattern from upstream to downstream, with higher spatial continuity in the plains than in the mountainous areas.

(3) Analysis of the dominant factors revealed significant differences in how various meteorological elements affect soil moisture at different scales. At the monthly scale, soil moisture was primarily controlled by precipitation, accounting for 36.62% of the variance, whereas at the weekly scale, VPD was dominant, contributing 47.04%. During drought events, as precipitation replenishment remains limited, the dominant role of monthly precipitation decreases substantially, whereas its relative contribution to evapotranspiration increases. However, on a weekly scale, the VPD consistently maintained absolute dominance as the key driver of rapid soil moisture depletion. These findings highlight a shift in the soil moisture control mechanisms from supply dominance to evapotranspiration consumption dominance under drought conditions.

This study analyzed soil moisture variations in the Yangtze River Basin across annual, monthly, and weekly scales and among the upper, middle, and lower reaches. Using a GAM, we quantified the relative effects of precipitation, temperature, wind speed, and VPD and examined how dominant factors changed during extreme drought events. The results provide scientific evidence for a scale-dependent soil moisture control mechanism in humid monsoon basins. Monthly soil moisture variations are mainly governed by precipitation recharge, whereas weekly variations are more strongly controlled by atmospheric evaporative demand, especially VPD. This finding improves the understanding of drought formation by showing that soil moisture drought cannot be explained by rainfall deficit alone. From a practical perspective, drought monitoring based only on precipitation may fail to detect rapid soil drying during hot and dry periods. Incorporating VPD, temperature, and other evapotranspiration-related variables can therefore improve drought diagnosis and early warning, and can support irrigation scheduling, reservoir operation, ecological water allocation, and adaptive water resource management in the Yangtze River Basin.

Author Contributions: Conceptualization, B.Z. and L.D.; methodology, Y.L.; validation, Y.L., R.H. and B.Z.; formal analysis, Y.L.; data curation, R.H.; writing—original draft preparation, Y.L.; writing—review and editing, R.H.; project administration, L.D. All authors have read and agreed to the published version of the manuscript.

Funding: This research was funded by grants from the National Natural Science Foundation of China (42301033, 42501052). This work was also funded by the research program of China Yangtze River Power Co., Ltd. (2425020015).

Institutional Review Board Statement: Not applicable.

Informed Consent Statement: Not applicable.

Data Availability Statement: The data that support the findings of this study are available on request from the corresponding author.

Conflicts of Interest: Author Lele Deng is employed by the company China Yangtze Power Co., Ltd. The remaining authors declare that the research was conducted in the absence of any commercial or financial relationships that could be construed as a potential conflict of interest.

References

1. Vereecken, H.; Amelung, W.; Bauke, S.L.; Bogena, H.; Brüggemann, N.; Montzka, C.; Vanderborght, J.; Bechtold, M.; Blöschl, G.; Carminati, A.; et al. Soil hydrology in the Earth system. *Nat. Rev. Earth Environ.* **2022**, *3*, 573–587. [CrossRef]
2. Seneviratne, S.I.; Corti, T.; Davin, E.L.; Hirschi, M.; Jaeger, E.B.; Lehner, I.; Orlowsky, B.; Teuling, A.J. Investigating soil moisture-climate interactions in a changing climate: A review. *Earth Sci. Rev.* **2010**, *99*, 125–161. [CrossRef]
3. Feng, H.; Zhang, M. Global land moisture trends: Drier in dry and wetter in wet over land. *Sci. Rep.* **2015**, *5*, 18018. [CrossRef] [PubMed]

4. McColl, K.A.; Alemohammad, S.H.; Akbar, R.; Konings, A.G.; Yueh, S.; Entekhabi, D. The global distribution and dynamics of the surface soil moisture. *Nat. Geosci.* **2017**, *10*, 100–104. [CrossRef]
5. He, N.; Guo, W.; Lan, J.; Yu, Z.; Wang, H. The impact of human activities and climate change on eco-hydrological processes in the Yangtze River basin. *J. Hydrol. Reg. Stud.* **2024**, *53*, 101753. [CrossRef]
6. Zehe, E.; Becker, R.; Bárdossy, A.; Plate, E. Uncertainty of simulated catchment runoff response in the presence of threshold processes: Role of initial soil moisture and precipitation. *J. Hydrol.* **2005**, *315*, 183–202. [CrossRef]
7. Vicente-Serrano, S.M.; Beguería, S.; López-Moreno, J.I. A Multiscalar Drought Index Sensitive to Global Warming: The Standardized Precipitation Evapotranspiration Index. *J. Clim.* **2010**, *23*, 1696–1718. [CrossRef]
8. Gu, L.; Schumacher, D.L.; Wang, H.M.; Yin, J.; Fischer, E.M. Land-atmosphere feedbacks drive dryland drought and expansion under climate warming. *Innovation* **2025**, *6*, 100863. [CrossRef] [PubMed]
9. Guswa, A.J. Canopy vs. roots: Production and destruction of variability in soil moisture and hydrological fluxes. *Vadose Zone J.* **2012**, *11*, vzj2011.0159. [CrossRef]
10. Gaur, N.; Mohanty, B.P. Evolution of physical controls for soil moisture in humid and sub-humid watersheds. *Water Resour. Res.* **2013**, *49*, 1244–1258. [CrossRef]
11. Ochsner, T.E.; Cosh, M.H.; Cuenca, R.H.; Dorigo, W.A.; Draper, C.S.; Hagimoto, Y.; Kerr, Y.H.; Larson, K.M.; Njoku, E.G.; Small, E.E.; et al. State of the art in large-scale soil moisture monitoring. *Soil Sci. Soc. Am. J.* **2013**, *77*, 1888–1919. [CrossRef]
12. Dorigo, W.; Himmelbauer, I.; Aberer, D.; Schremmer, L.; Petrakovic, I.; Zappa, L.; Preimesberger, W.; Xaver, A.; Annor, F.; Ardö, J.; et al. The International Soil Moisture Network: Serving Earth system science for over a decade. *Hydrol. Earth Syst. Sci.* **2021**, *25*, 5749–5804. [CrossRef]
13. Liu, W.; Wang, J.; Xu, F.; Li, C.; Xian, T. Validation of four satellite-derived soil moisture products using ground-based in situ observations over Northern China. *Remote Sens.* **2022**, *14*, 1419. [CrossRef]
14. Wu, Q.; Liu, H.; Wang, L.; Deng, C. Evaluation of AMSR2 soil moisture products over the contiguous United States using in situ data from the International Soil Moisture Network. *Int. J. Appl. Earth Obs. Geoinf.* **2016**, *45*, 187–199. [CrossRef]
15. Dorigo, W.; Wagner, W.; Albergel, C.; Albrecht, F.; Balsamo, G.; Brocca, L.; Chung, D.; Ertl, M.; Forkel, M.; Gruber, A.; et al. ESA CCI Soil Moisture for improved Earth system understanding: State-of-the art and future directions. *Remote Sens. Environ.* **2017**, *203*, 185–215. [CrossRef]
16. Zhu, L.; Wang, H.; Tong, C.; Liu, W.; Du, B. Evaluation of ESA active, passive and combined soil moisture products using upscaled ground measurements. *Sensors* **2019**, *19*, 2718. [CrossRef] [PubMed]
17. Davarzani, H.; Smits, K.; Tolene, R.M.; Illangasekare, T. Study of the effect of wind speed on evaporation from soil through integrated modeling of the atmospheric boundary layer and shallow subsurface. *Water Resour. Res.* **2014**, *50*, 661–680. [CrossRef] [PubMed]
18. Yuan, W.; Zheng, Y.; Piao, S.; Ciais, P.; Lombardozzi, D.; Wang, Y.; Ryu, Y.; Chen, G.; Dong, W.; Hu, Z.; et al. Increased atmospheric vapor pressure deficit reduces global vegetation growth. *Sci. Adv.* **2019**, *5*, eaax1396. [CrossRef] [PubMed]
19. Gu, X.; Jamshidi, S.; Sun, H.; Niyogi, D. Identifying multivariate controls of soil moisture variations using multiple wavelet coherence in the U.S. Midwest. *J. Hydrol.* **2021**, *602*, 126755. [CrossRef]
20. Novick, K.A.; Ficklin, D.L.; Stoy, P.C.; Williams, C.A.; Bohrer, G.; Oishi, A.; Papuga, S.A.; Blanken, P.D.; Noormets, A.; Sulman, B.N.; et al. The increasing importance of atmospheric demand for ecosystem water and carbon fluxes. *Nat. Clim. Change* **2016**, *6*, 1023–1027. [CrossRef]
21. Li, Y.X.; Leng, P.; Kasim, A.A.; Li, Z.L. Spatiotemporal variability and dominant driving factors of satellite observed global soil moisture data from 2001 to 2020. *J. Hydrol.* **2025**, *654*, 132848. [CrossRef]
22. Coleman, M.L.; Niemann, J.D. An evaluation of nonlinear methods for estimating catchment-scale soil moisture patterns based on topographic attributes. *J. Hydroinf.* **2012**, *14*, 800–814. [CrossRef]
23. Wood, S.N. *Generalized Additive Models: An Introduction with R*, 2nd ed.; Chapman and Hall/CRC: Boca Raton, FL, USA, 2017. [CrossRef]
24. Abolafia-Rosenzweig, R.; He, C.; Chen, F.; Ikeda, K.; Schneider, T.; Rasmussen, R. High resolution forecasting of summer drought in the Western United States. *Water Resour. Res.* **2023**, *59*, e2022WR033734. [CrossRef]
25. Xu, J.; Yang, D.; Yi, Y.; Lei, Z.; Chen, J.; Yang, W. Spatial and temporal variation of runoff in the Yangtze River basin during the past 40 years. *Quat. Int.* **2008**, *186*, 32–42. [CrossRef]
26. Ma, M.; Qu, Y.; Lyu, J.; Zhang, X.; Su, Z.; Gao, H.; Yang, X.; Chen, X.; Jiang, T.; Zhang, J.; et al. The 2022 extreme drought in the Yangtze River Basin: Characteristics, causes, and response strategies. *River* **2022**, *1*, 162–171. [CrossRef]
27. Wei, J.; Wang, Z.; Han, L.; Shang, J.; Zhao, B. Analysis of spatio-temporal evolution characteristics of drought and its driving factors in Yangtze River Basin based on SPEI. *Atmosphere* **2022**, *13*, 1986. [CrossRef]
28. Colliander, A.; Jackson, T.J.; Bindlish, R.; Chan, S.; Das, N.; Kim, S.B.; Cosh, M.H.; Dunbar, R.S.; Dang, L.; Pashaian, L.; et al. Validation of SMAP surface soil moisture products with core validation sites. *Remote Sens. Environ.* **2017**, *191*, 215–231. [CrossRef]
29. Wang, A.; Shi, X. A multilayer soil moisture dataset based on the gravimetric method in China and its characteristics. *J. Hydrometeorol.* **2019**, *20*, 1721–1736. [CrossRef]

30. Su, Z.; Zhang, H.; Li, X.; Wu, S.; Shi, M.; Luo, M. A high-resolution daily and 1 km atmospheric moisture collection over the North China Plain during 2003–2020. *Sci. Data* **2026**, *13*, 960. [CrossRef] [PubMed]
31. Wigneron, J.-P.; Calvet, J.-C.; Pellarin, T.; Van de Griend, A.A.; Berger, M.; Ferrazzoli, P. Retrieving near-surface soil moisture from microwave radiometric observations: Current status and future plans. *Remote Sens. Environ.* **2003**, *85*, 489–506. [CrossRef]
32. Zheng, J.; Zhao, T.; Lü, H.; Zou, D.; Rodriguez-Fernandez, N.; Mialon, A.; Richaume, P.; Xiao, J.; Ma, J.; Fan, L.; et al. Use of a new Tibetan Plateau network for permafrost to characterize satellite-based products errors: An application to soil moisture and freeze/thaw. *Remote Sens. Environ.* **2023**, *295*, 113899. [CrossRef]
33. Brocca, L.; Tullo, T.; Melone, F.; Moramarco, T.; Morbidelli, R. Catchment-scale soil moisture spatial-temporal variability. *J. Hydrol.* **2012**, *422–423*, 63–75. [CrossRef]
34. McVicar, T.R.; Roderick, M.L.; Donohue, R.J.; Li, L.T.; Van Niel, T.G.; Thomas, A.; Grieser, J.; Jhajharia, D.; Himri, Y.; Mahowald, N.M.; et al. Global review and synthesis of trends in observed terrestrial near-surface wind speeds: Implications for evaporation. *J. Hydrol.* **2012**, *416–417*, 182–205. [CrossRef]
35. Jung, M.; Reichstein, M.; Ciais, P.; Seneviratne, S.I.; Sheffield, J.; Goulden, M.L.; Bonan, G.; Cescatti, A.; Chen, J.; de Jeu, R.; et al. Recent decline in the global land evapotranspiration trend due to limited moisture supply. *Nature* **2010**, *467*, 951–954. [CrossRef] [PubMed]
36. Fu, Z.; Ciais, P.; Prentice, I.C.; Gentine, P.; Makowski, D.; Bastos, A.; Luo, X.; Green, J.K.; Stoy, P.C.; Yang, H.; et al. Atmospheric dryness reduces photosynthesis along a large range of soil water deficits. *Nat. Commun.* **2022**, *13*, 989. [CrossRef] [PubMed]
37. Gamelin, B.L.; Feinstein, J.; Wang, J.; Bessac, J.; Yan, E.; Kotamarthi, V.R. Projected U.S. drought extremes through the twenty-first century with vapor pressure deficit. *Sci. Rep.* **2022**, *12*, 8615. [CrossRef] [PubMed]